Electronic Supplementary Material (ESI) for Journal of Materials Chemistry C.

Interdependence of Shape and Magnetic Properties in Al-nanoparticles doped with Ni and Pt

Omar López-Estrada
Departamento de Física y Química Teórica, Facultad de Química, Universidad Nacional Autónoma de México, Cd. Universitaria, CP 04510, Ciudad de México, México and Physics Department, King's College London, WC2R 2SL, London

Emilio Orgaz
Departamento de Física y Química Teórica, Facultad de Química, Universidad Nacional Autónoma de México, Cd. Universitaria, CP 04510, Ciudad de México, México

Francesca Baletto
Physics Department, King's College London, WC2R 2SL, London

BOMD SIMULATIONS DETAILS

The BOMD simulations details are described below.

In the doublet spin state of Ni@centre the dIh evolves towards a distorted Dh+Th$_{cp}$ structure within $\approx$ 1 ps (Fig. S2), the severe structural transformation is reflected by a drop to zero of the (5,5,5) CNA-signature and the appearance of 5 $\sim$ 15% of the (4,2,2) signature (Fig. S4 top panel left). The structural transformation of the dIh in the doublet spin state of Pt@centre is slower (Fig. S3). A breathing, in the first ps, is followed by the distortion of the perfect dIh with a drop of the (5,5,5) signature (Fig. S6 top panel left), then a momentary appearance of the (4,2,2) and (4,2,1) signatures to later achieve a recover of the (5,5,5) signature to almost 20%. This interchange between the three signatures lasted 3 ps, to reach an equilibrium of the (5,5,5) signature slightly above 10%. The outcome structural motif loses its 4 atoms long axis and can be seen, in contrast as in the Ni case, as a very distorted Ih+Oh.

Energetically above, we observed the distorted Ni@centre Dh+Th$_{cp}$ (Fig. S2) in a quadruplet spin state and the M=8 spin multiplicity of Pt@centre Dh+Th$_{cp}$. The Ni-doped structure evolution shows a breathing followed by the vibration of the apex Al atoms within $\approx$ 2 ps. It has an almost 35% lost of the (5,5,5) signature and the provisional appearance of $\approx$ 10% of the (4,2,2) signature, and at the end both signatures are below 5% (Fig. S4). Pt@centre cluster evolves toward a Dh+Th$_{cp}$ without the complete lose of the (5,5,5) signature, and a gradual appearance of the (4,2,2) signature is observed. This is reflected in the formation of a Dh and the (111) facets that remains in the cluster. It is to notice that the 4 atoms long are not maintained in the axis and the occurrence of a displacement of some aluminum atoms is to allow that a Pt atom is exposed on the surface of the cluster. Both signatures, the (5,5,5) and the (4,2,2) appear to be noisy but in average they remain below 5% an 15% respectively.

A similar behaviour is exhibited for the M=6 and 8 Ni@centre spin multiplicities. Energetically both preserves the dIh motifs, although higher in energy to the previous structures described. In average, the M= 6 spin state is lower in energy than the M= 8 spin state (Fig. S2). During the dynamics of both systems, there is a breathing of the penta–rings corresponding to the sudden appearance of the (4,2,2) (Fig. S4 bottom panel left and right), and the temporary lost of a few nearest neighbours leading to the momentary fading of the (111) facets.

Pt@vertex nanoalloy with M=4 and M=6 evolves toward a slightly distorted dIh characterised by a breathing of the structural motif with an elongation of the central axis and a distortion of the pentagonal rings, with a net reduction of the overall coordination.

Pt@vertex, with the M=4 and 6 spin state multiplicities imposed, evolve toward a distorted dIh (Fig. S3 panel right). The first exhibits an elongation of the 4 atoms long followed by the distortion of the penta-rings losing at least one bond in each of them. There is still an Ih shape reflected in the high initial (5,5,5) signature (Fig. S7 top panel right) to continue after 2 ps fluctuating in average around 15%. Although there exists the appareance of the (4,2,2) signature (>5%) it is not observed a structure near to the Dh below the Ih. The second shows an elongation of the 4 atoms long preserving the 5–fold axis but losing many first neighbours bonds of the penta–rings, confirmed by the CNA (see Fig. S7 bottom panel left) where it is observed a gradual loss of the (5,5,5) signature within 1ps and the appearance of the (4,2,2) signature within 1 – 2ps of the simulation. Then a slight noise of both, the (5,5,5) and the (4,2,2) signatures was preserved along the simulation around 10% and 5% respectively.

Ni@vertex in a doublet spin state is close in energy to the Ni@centre simulation with the M= 8 imposed (Fig. S2). The dIh evolves toward a dDh by a twist of the "ABA" penta–rings to an "AAA" ordering conserving the 4 atoms long axis. It is to note that the structure change toward a dDh mediated by the Ni atoms was not observed in the Pt-doping BOMD simulations. The structure evolution leads to the disappearance of the (111) facets to form a dDh (0.5 $\sim$ 1.5 ps) and then a dDh sp , demonstrated for the 10$\sim$15% increasing of the (4,2,2) signature (Fig. S5 top panel left) resulting in the formation of the (100) facets.

Ni@vertex for the M= 4 – 8 spin multiplicities and Pt@vertex for the M=2 and 8 spin multiplicities exhibit a Ih+Dh in their respectively energy trajectories. The dIh Ni@vertex quadruplet spin state exhibits a breathing followed by a momentary spiral distortion of the penta–rings "ABA" to reach the gradual reordering "AAB" within 1 ps. This Ih+Dh had a sharp fall of the (5,5,5) signature (Fig. S5 top panel right) allowing the fast formation of the (100) facets. An oscilation observed in the central aluminums is reflected in the (4,2,2) noisy signature (between 5$\sim$20%), this resulting in the disappearance on the fly of the (111) facets of the top Ih and the durable <5% of the (5,5,5) signature.

The dIh Ni@vertex in a sextuplet spin state exhibits a fast lost of the (5,5,5) signature, followed by the formation

of the (4,2,2) signature ($\approx$ 10%) observed in the rearrangement of the penta–rings ABA to reach an AAB ordering (Fig. S2 panel right), the low (5,5,5) signature along the simulation is preserved and the formation of (100) facets is confirmed by the (4,2,2) signature (5 $\sim$ 10%). In comparison with the previous structures, this Ih+Dh shows a less noisy (4,2,2) signature because of an elongation of the whole bond cluster.

In the case of the M=8 spin state Ni@vertex, the structural transformation is at first instance a breathing along the 4 atoms long axis, which bring to the lost of any (5,5,5) signature (Fig. S5 bottom panel right). A momentary occurrence of a dDh shape is observed within 1 ps, confirmed by the fast appearance of the (4,2,2) signature ($\approx$ 20%). This occurrence is reflected in the briefly "AAA" ordering of the penta–rings to reach later an "AAB" ordering. This Ih+Dh is more expanded than the sextuplet Ih+Dh, explained by the low signatures (Fig. S5) observed in the CNA (<5% for the (5,5,5) signature), and a slightly oscillation around 5% of the (4,2,2) signature.

For Pt@vertex, the doublet spin state shows a reordering of the penta–rings within 2 ps (Fig. S3 panel right). The 4 atoms long axis is preserved just being slightly distorted, but the rotation of the penta–rings yields the distorted Ih+Dh. The CNA exhibited this Ih+Dh in the signatures, in average the (5,5,5) signature above 10% and the (4,2,2) signature above 5% during the entire simulation (see Fig. S7 top panel left). In the case of the M=8 multiplicity, it exhibits a slight breathing and then a gradual rotation of one penta–ring. In the same way the CNA confirms the Ih+Dh shape observed, where a well defined 20% and $\approx$ 15% of the (5,5,5) and (4,2,2) signatures respectively are observed along the simulation.

For the Pt@centre quadruplet spin state BOMD simulation, it is observed the evolution towards a distorted Ih+Oh (Fig. S3 panel left). The structural transformation from the dIh is a first breathing lasting almost 3 ps, when the lose of the (5,5,5) signature until 0% took place (Fig. S6 top panel right). In the same time interval the appearance of the (4,2,2) signature occurres to achieve a 10 $\sim$ 15% of this signature. Approximately after 3 ps an invariant trend of both signatures is observed. The (5,5,5) signature remains between a noisy 5% to $\approx$ 10%, and the (4,2,2) signature is shown below 5%. A very slight appearance of the FCC (4,2,1) signature is also observed. Another case of a distorted Ih+Oh structure is the M= 6 spin multiplicity of Pt@centre (Fig. S3 panel left). The breathing of the structure is observed within 1 ps. This is an elongation of the 4 atoms long along with the separation of the penta–rings. This separation allows the lose of the (5,5,5) signature (Fig. S6 bottom panel left) followed by the momentary formation of (100) facets and then the final distortion of the 4 atoms long axis. One of the Pt atoms is observed to displace to the surface of the cluster remaining bonded to the second Pt atom. A regular trend is achieved after 5 ps, being the (5,5,5) signature in average around 5% and the (4,2,2) signature below 10 %.

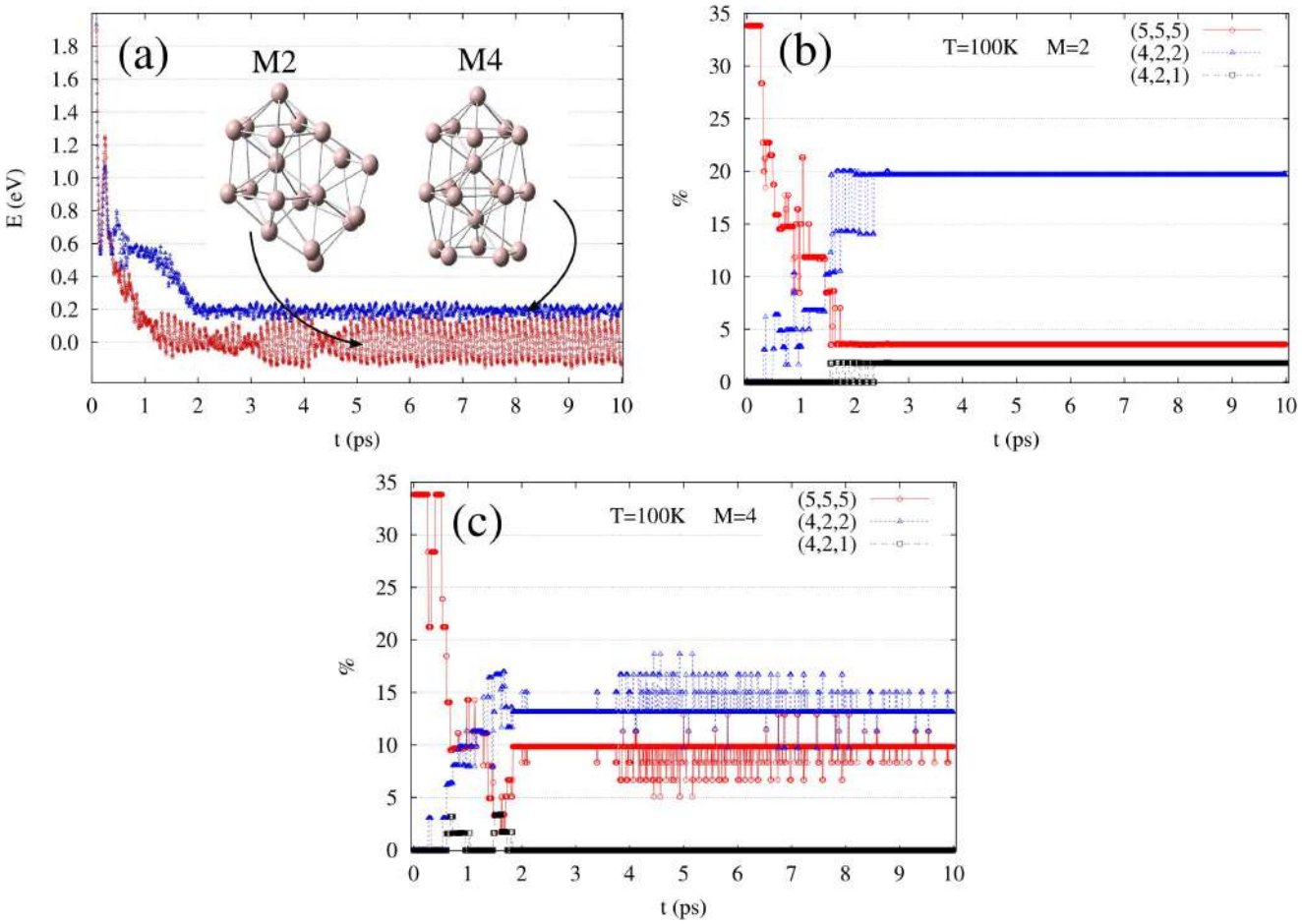

Fig. S1. (a) Born–Oppenheimer molecular dynamics simulations at 100 K for Al_{19} at the PBE/SDecp theory level. Snapshots of the structure evolution for the doublet and quadruplet spin multiplicities are indicated. Common neighbour analysis of the BOMD simulations at doublet (b) and quadruplet (c) spin multiplicities.

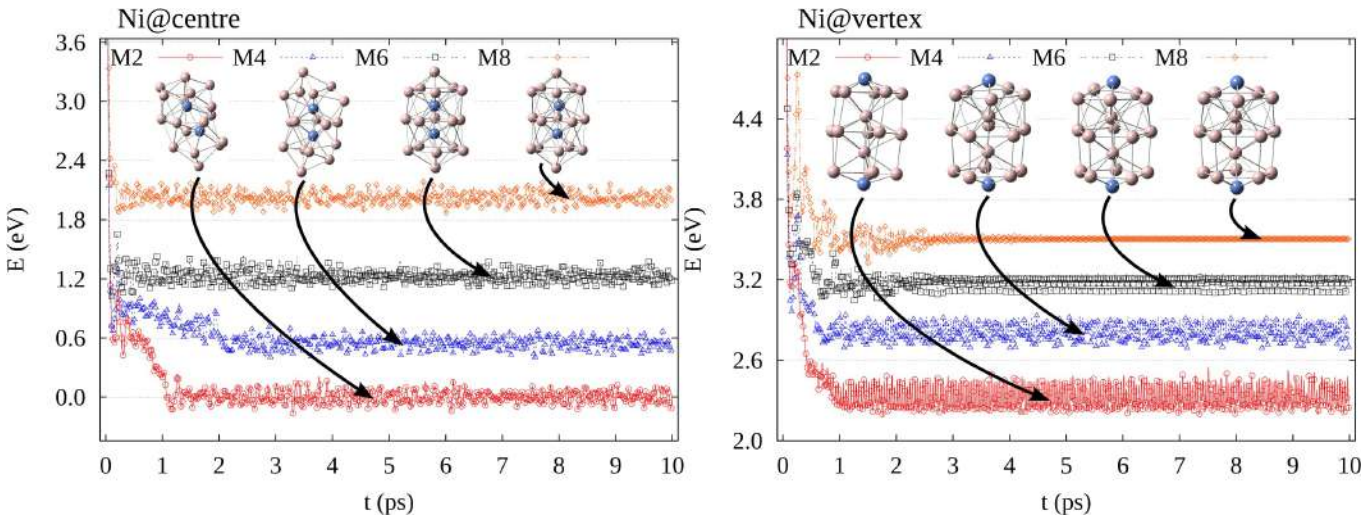

Fig. S2. Born–Oppenheimer molecular dynamics trajectories at 100 K for $Al_{17}Ni_2$ for Ni at centre and vertex as impurities of the Al_{19} double icosahedral structure at the PBE/SDecp theory level. Different spin multiplicities (M) are indicated. The 0.0 eV reference is the average energy from 4 – 10 ps of the doublet spin state for Ni at centre.

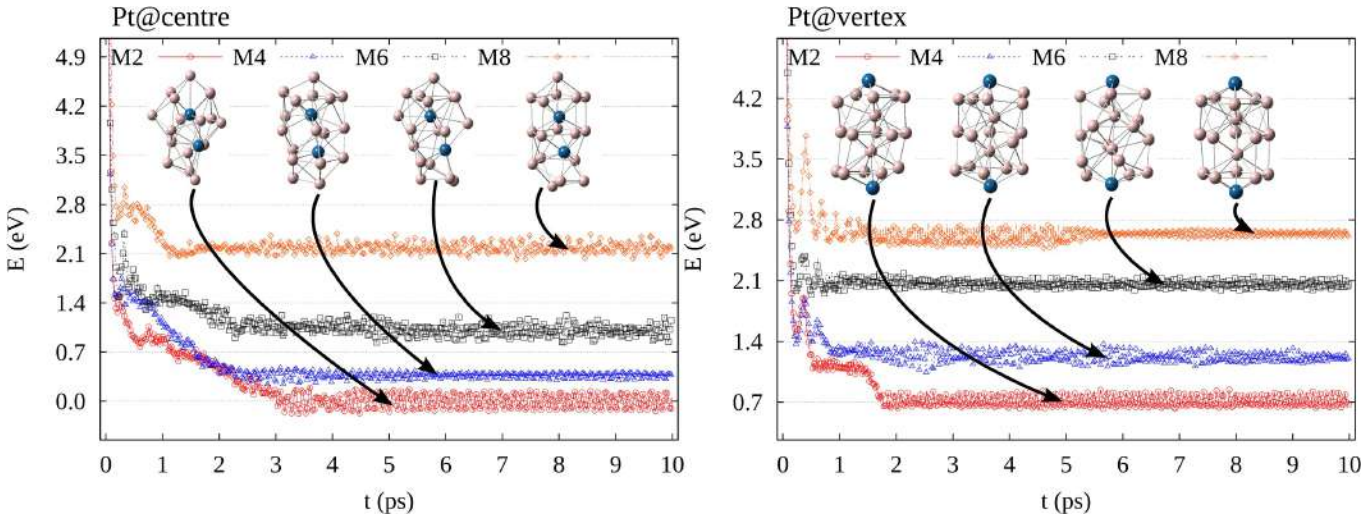

Fig. S3. Born–Oppenheimer molecular dynamics trajectories at 100 K for $Al_{17}Pt_2$ Pt at centre and vertex as impurities of the Al_{19} double icosahedral structure at the PBE/SDecp theory level. Different spin multiplicities (M) are indicated. The 0.0 eV reference is the average energy from 4 – 10 ps of the doublet spin state for Pt at centre.

TABLE – S1 –: Total magnetization (M in μ_B), absolute magnetization (|M| in μ_B) and energetic stability with respect to the dIh (Δ E= in meV/atom) using QuantumEspresso package and two different functionals (PBE, PBESol) and both US, PAW pseudo-potentials for the decahedron capped (Dh_{cp}), the dadaist double-decahedron (dDh_{dd}) and the double icosahedron (dIh).

	$Dh+Th_{cp}$			Dh_7+Hex			dIh		
	M	|M|	Δ E	M	|M|	Δ E	M	|M|	Δ E
PBE US	1.0	1.35	-20.0	3.0	3.33	-12.0	5.0	5.54	0.0
PBESol US	1.0	1.27	-20.0	3.0	3.25	-13.0	5.0	5.54	0.0
PBE PAW	1.0	1.34	-21.0	3.0	3.32	-13.0	5.0	5.54	0.0
PBESol PAW	1.0	1.27	-23.0	3.0	3.25	-16.0	3.0	4.32	0.0

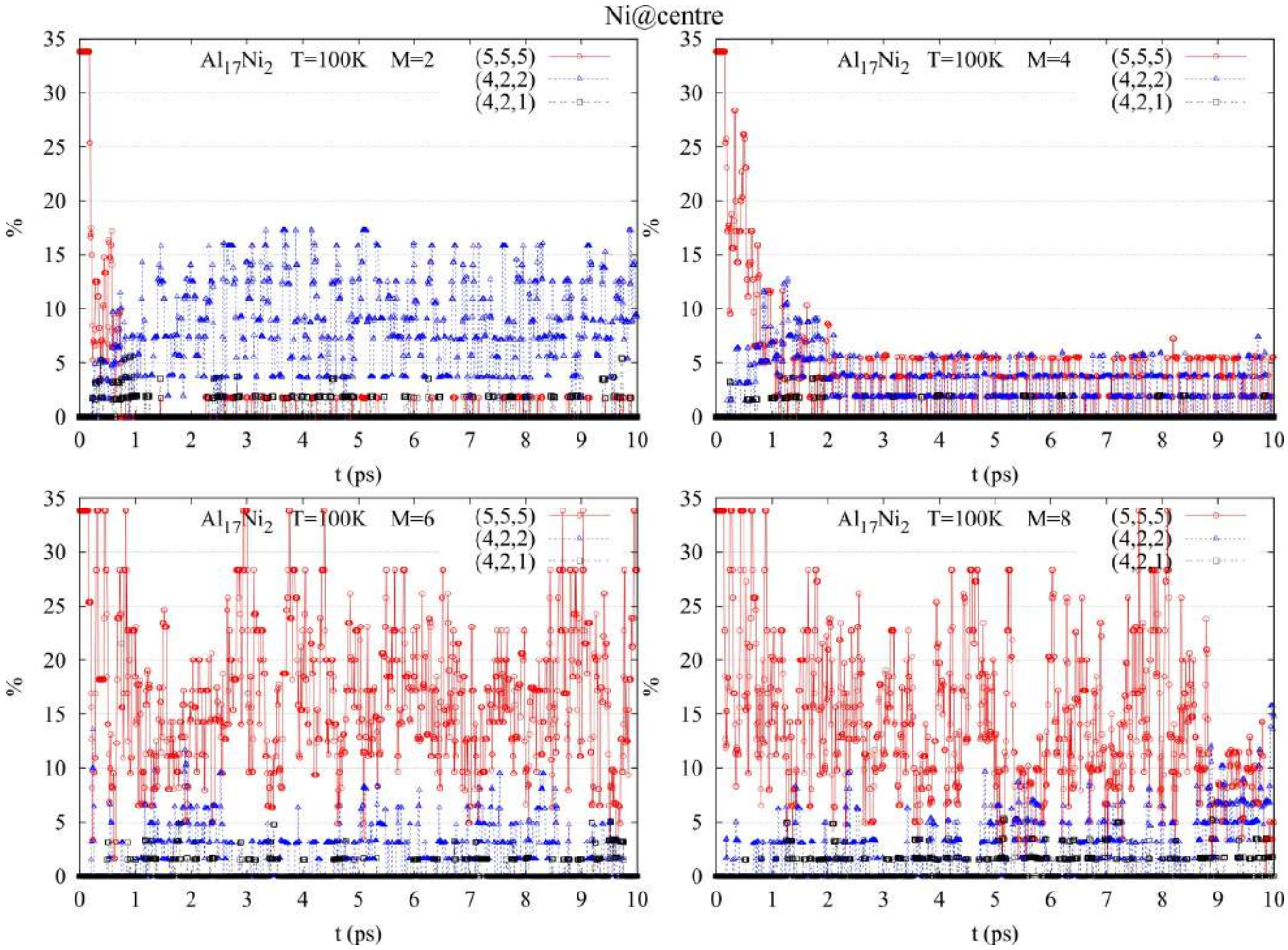

Fig. S4. Common neighbour analysis for the BOMD trajectories of $Al_{17}Ni_2$ (Ni at centre) at T=100K for M= $2, 4, 6, 8$ spin multiplicities.

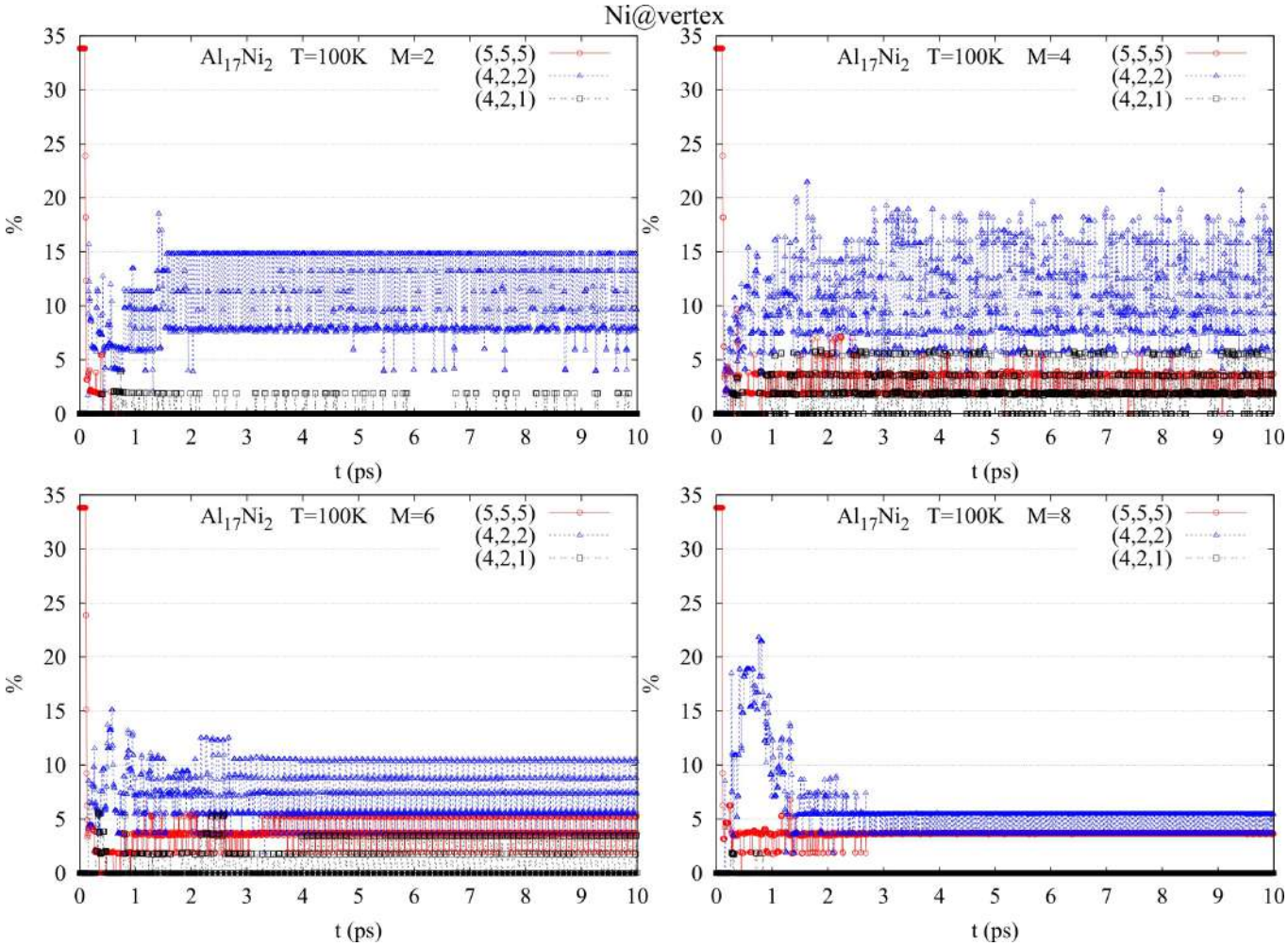

Fig. S5. Common neighbour analysis for the BOMD trajectories of $Al_{17}Ni_2$ (Ni at vertex) at T=100K for M= $2, 4, 6, 8$ spin multiplicities.

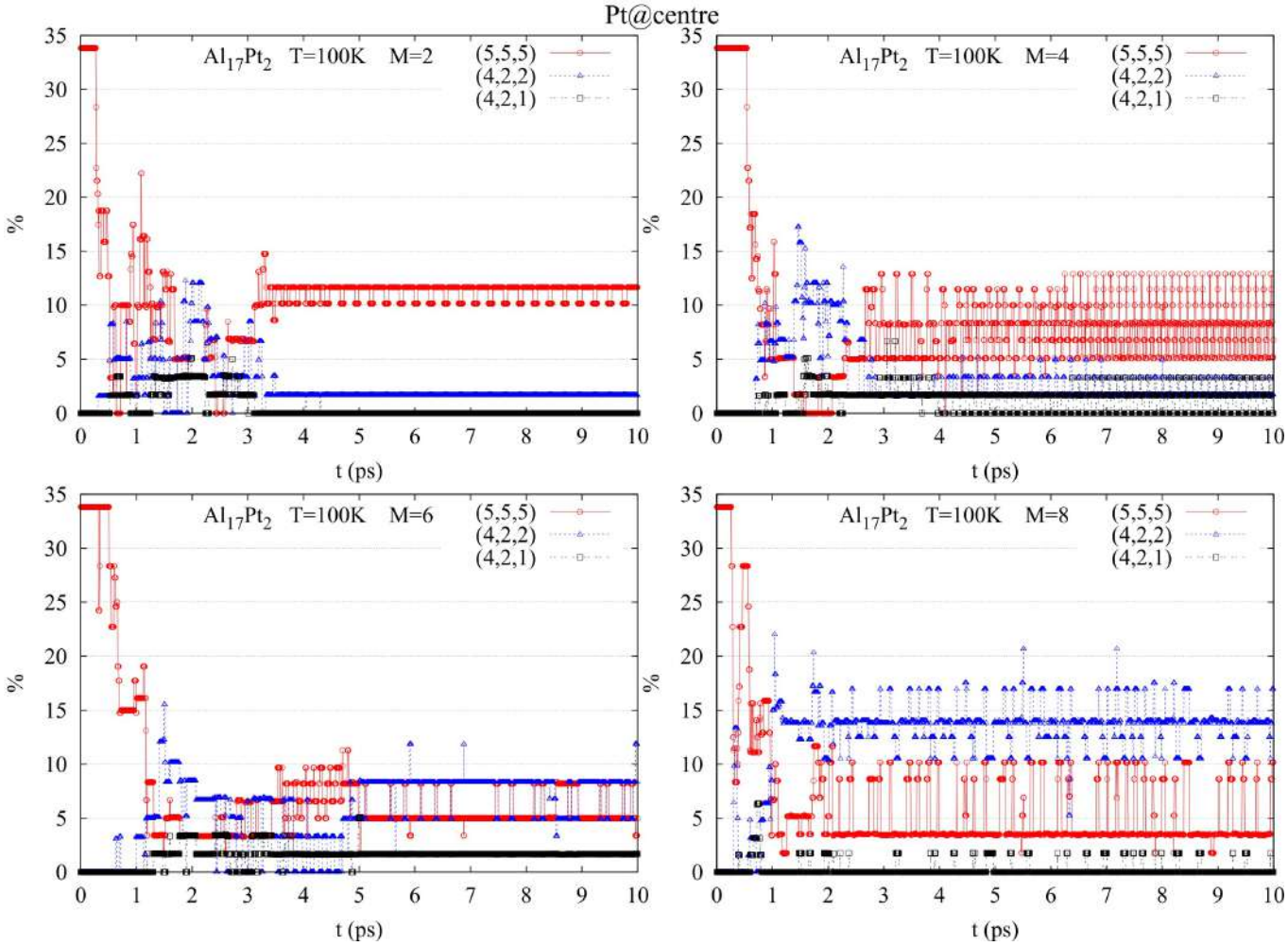

Fig. S6. Common neighbour analysis for the BOMD trajectories of $Al_{17}Pt_2$ (Pt at centre) at T=100K for M= $2, 4, 6, 8$ spin multiplicities.

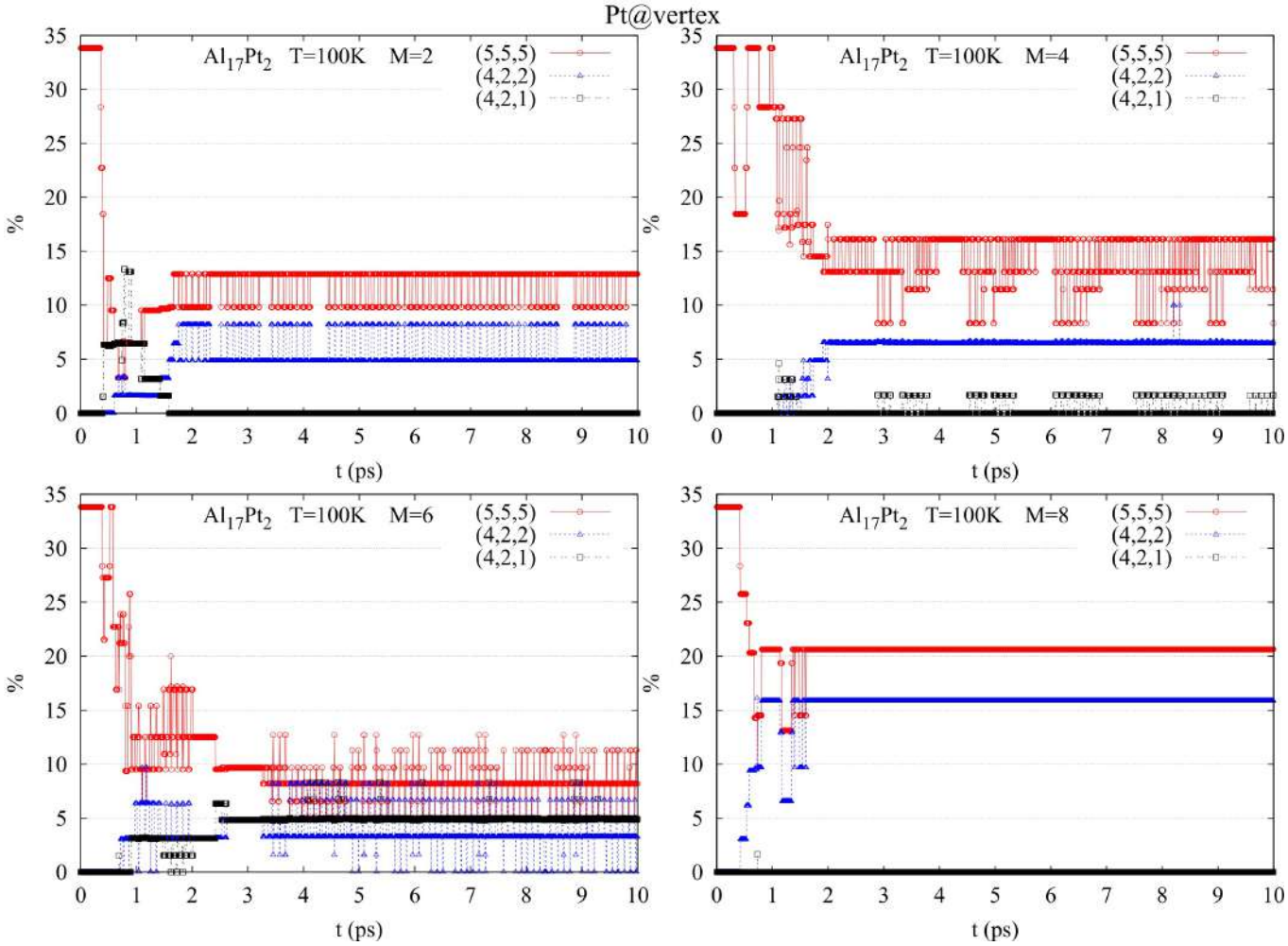

Fig. S7. Common neighbour analysis for the BOMD trajectories of $Al_{17}Pt_2$ (Pt at vertex) at T=100K for M= $2, 4, 6, 8$ spin multiplicities.

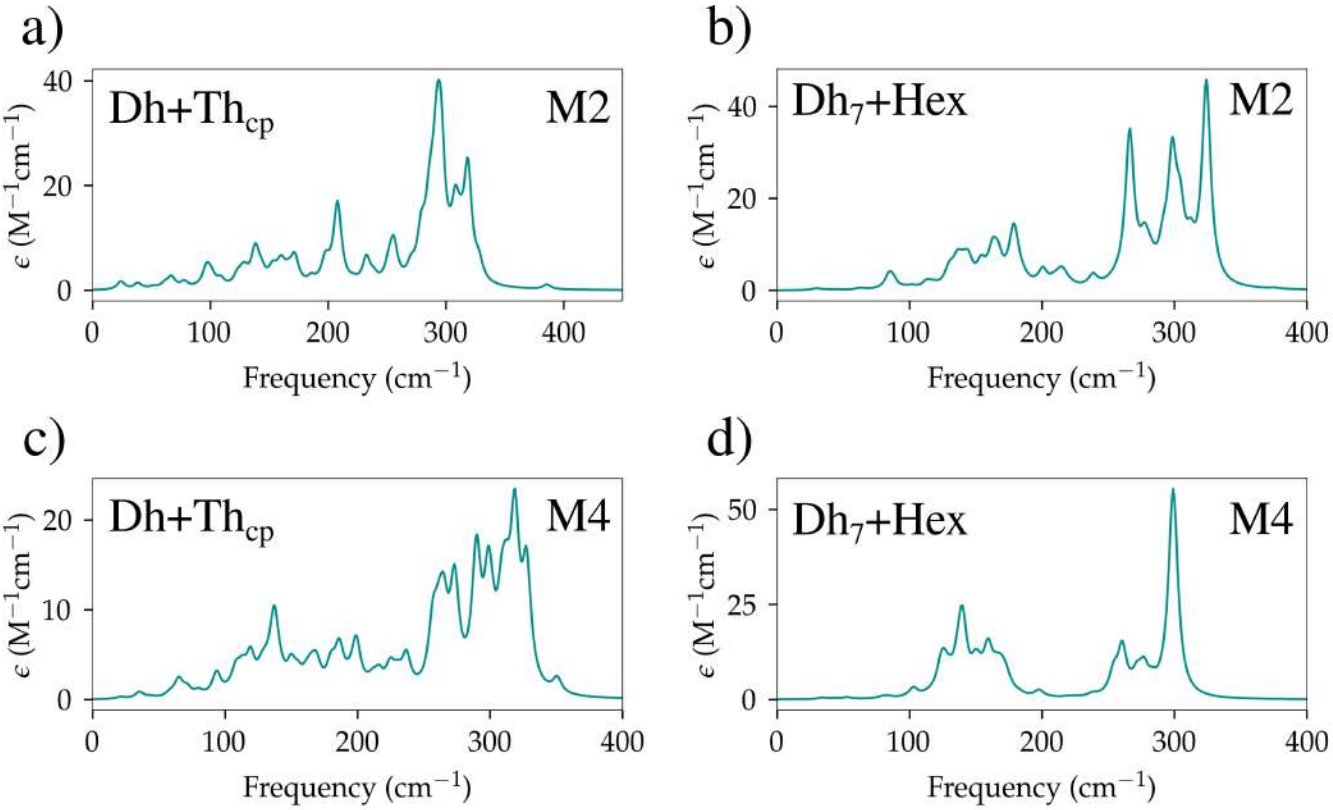

Fig. S8. Infrared spectra of Al_{19} for M= 2, 4 spin multiplicities. The corresponding structures are indicated and refer to the Fig 3 in the main manuscript.

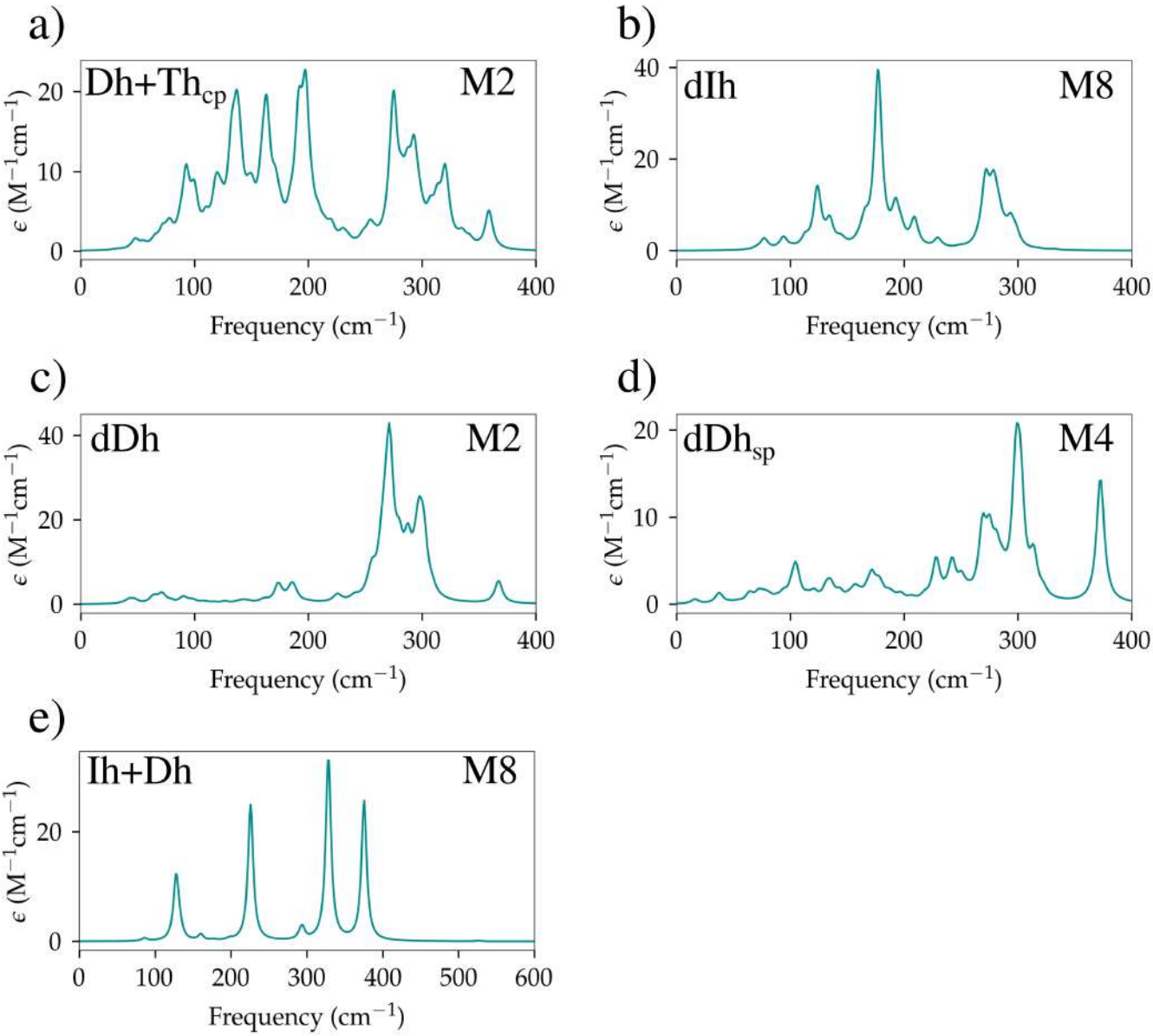

Fig. S9. Infrared spectra of representative $Al_{17}Ni_2$ structures for M= 2, 4, 8 spin multiplicities. In structure b), nickel is located in the centre, in c), d) and e) in the vertex.

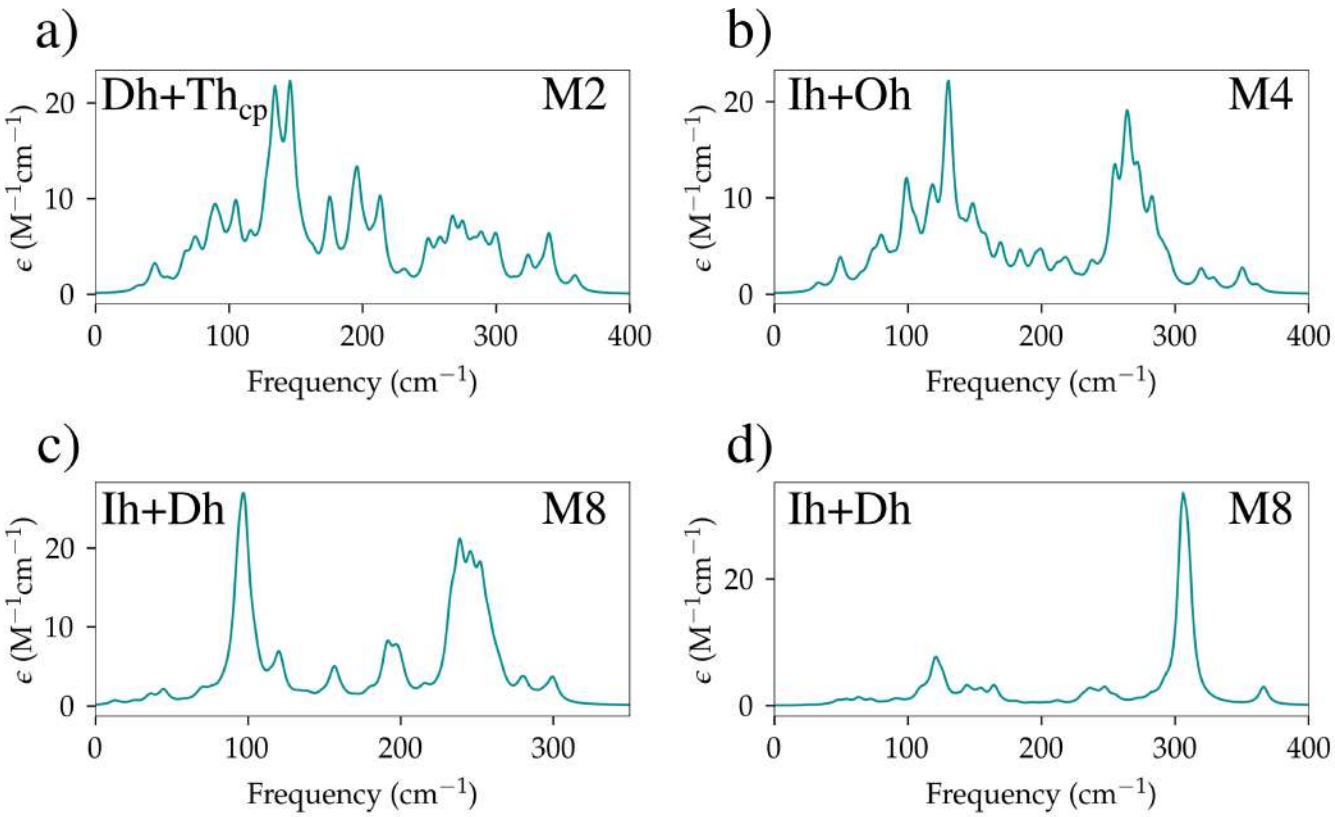

Fig. S10. Infrared spectra of representative $Al_{17}Pt_2$ structures for M= 2, 4, 8 spin multiplicities. In structures b) and c), platinum is located in the centre, in d) in the vertex.

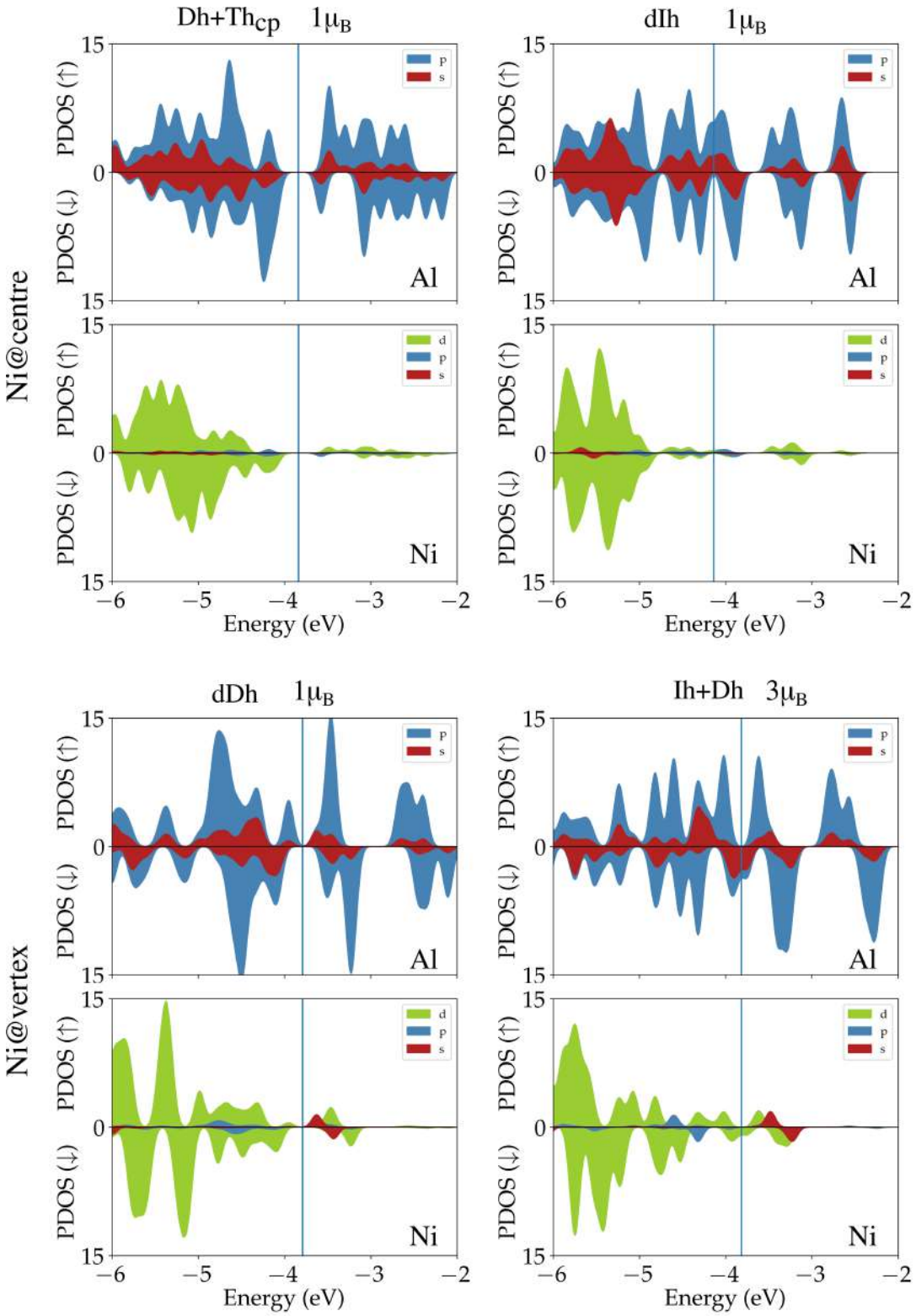

Fig. S11. Projected Density of States (PDOS) of representative $Al_{17}Ni_2$ structures. Al and Ni s,p,d states are plotted separately for each structure. A Gaussian broadening of 0.08 eV has been employed. The vertical line is in the average of the HOMO and LUMO energies for majority (↑) and minority spin (↓). The minority spin is shifted to be at same level of energy as the majority spin for easy comparison between different structures.

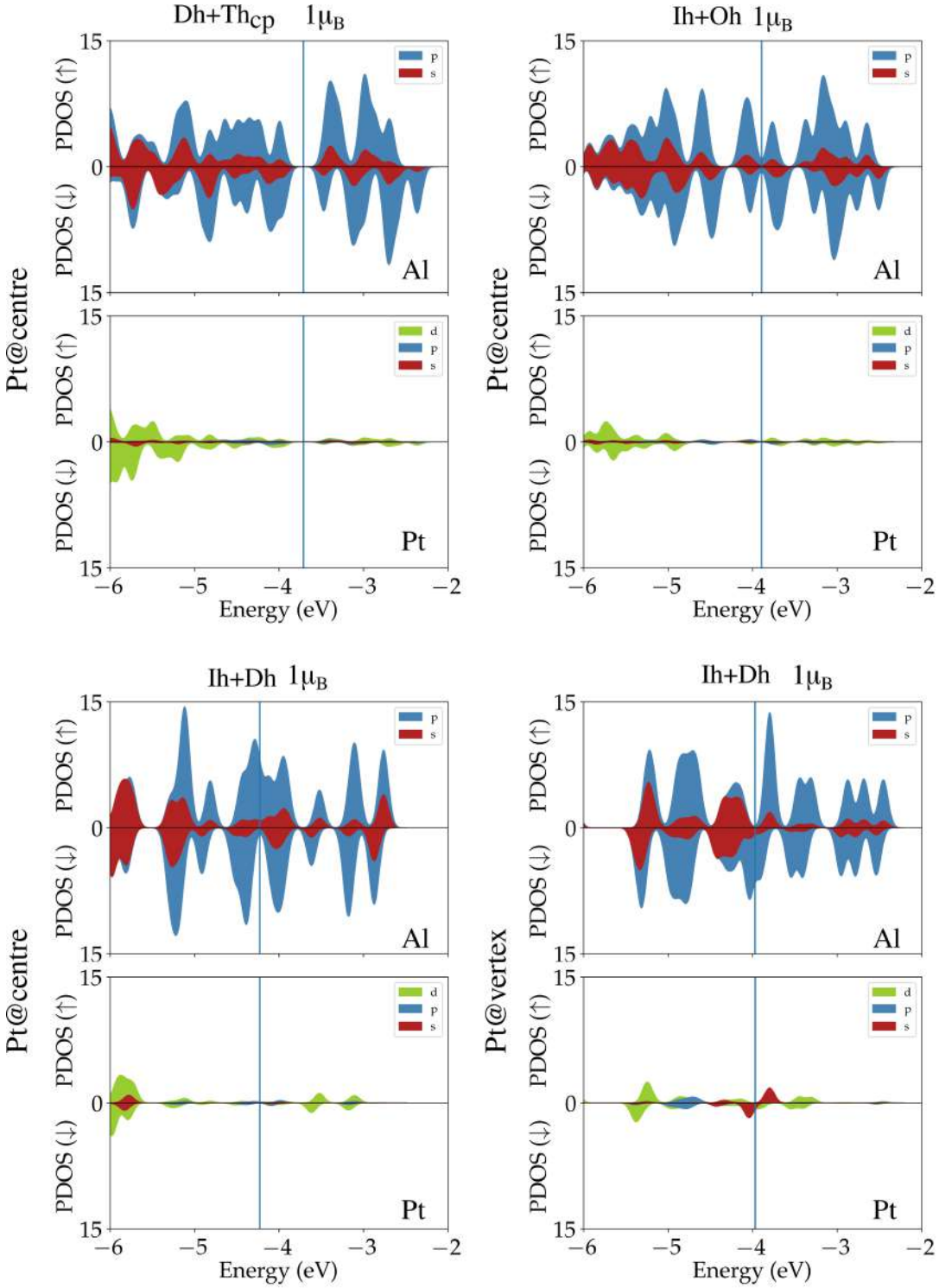

Fig. S12. Projected Density of States (PDOS) of representative $Al_{17}Pt_2$ structures. Al and Pt s,p,d states are plotted separately for each structure. A Gaussian broadening of 0.08 eV has been employed. The vertical line is in the average of the HOMO and LUMO energies for majority (↑) and minority spin (↓). The minority spin is shifted to be at same level of energy as the majority spin for easy comparison between different structures.

XYZ COORDINATES OF REPRESENTATIVE STRUCTURES

19
$Dh+Th_{cp}$

Al	1.22781000	-0.66589100	-3.78602900
Al	0.72102000	-0.50053400	3.83649300
Al	-1.50531600	0.74681700	-3.34766000
Al	-0.23896200	2.77816600	-2.06402000
Al	-2.08567200	-1.80596700	-2.61336700
Al	2.12051800	1.66486500	-2.76783100
Al	0.40715700	-2.89129800	-2.41200400
Al	-2.72867500	0.27289700	2.06815800
Al	-0.85865300	1.74608200	3.21344900
Al	-1.14674800	-2.20434500	2.71315100
Al	1.96496000	1.79002600	2.63395600
Al	2.48918200	-1.07423700	1.84732000
Al	-2.12227400	1.08521100	-0.47589200
Al	-2.00163500	-1.75408900	0.11122700
Al	0.04184000	2.79365600	0.78206000
Al	0.80748300	-2.63239300	0.33569000
Al	2.41398500	0.95186300	-0.05838100
Al	0.04205600	0.03688400	1.25702400
Al	0.45192500	-0.33771200	-1.27334200

19
Dh_7+Hex

Al	1.09003288	-1.66516447	-3.17668718
Al	0.44585677	-0.31508970	4.07242343
Al	-2.59800586	0.87148754	-2.62832102
Al	-0.34729791	2.62201748	-2.73331385
Al	-1.64408074	-1.74138865	-2.89894262
Al	1.92692024	0.97337071	-3.10729864
Al	2.39188353	-1.18550840	-0.63316680
Al	-2.06005130	-0.95443463	2.64769959
Al	-1.18697176	1.76494954	2.71783542
Al	0.29651275	-2.65885192	2.29662982
Al	1.63340012	1.84819869	2.42573725
Al	2.62815120	-0.84681618	2.16766868
Al	-2.46007362	1.20076377	0.19029487
Al	-2.29379184	-1.51502686	-0.11949845
Al	-0.16795293	2.72744794	0.10135556
Al	0.12704676	-2.68374292	-0.53613364
Al	2.26624113	1.52617431	-0.34063371
Al	0.13140544	-0.13666211	1.04116949
Al	-0.17922485	0.16827687	-1.48681719

19
Dh+Th$_{cp}$ Ni
Al -2.68529500 -0.23381600 2.35743100
Al 0.68753400 2.25256200 2.06309100
Al -0.83681800 -2.38851100 1.74294500
Al 2.36474900 0.14831800 2.47135800
Al 1.33847200 -2.28743900 3.26532300
Ni 0.05498500 -0.31306300 1.09369300
Al -2.49761900 -0.97372200 -0.16804300
Al -1.46036700 1.52658200 0.52396400
Al 0.40065700 3.04031900 -0.61592200
Al 2.00441600 -2.10155300 0.60928700
Al 2.00681200 0.82476200 -0.06213900
Ni -0.32079300 0.35365700 -1.22896000
Al -1.33509700 2.49304500 -2.65857100
Al -2.21143600 -0.05866800 -2.80567200
Al -0.28314600 -2.22121700 -0.91614600
Al 1.30858500 1.58806400 -2.96061900
Al 1.92682000 -1.15038700 -1.98014400
Al -0.26847300 -0.00342400 3.51885400
Al 0.11842200 -0.54322100 -4.09074800

19
dIh Ni Centre
Al -2.27095175 0.04473925 2.42512474
Al -0.84627310 2.45328599 2.53398929
Al -0.69479973 -2.30215891 2.41459255
Al 1.74758718 1.39963230 2.43065256
Al 1.91769409 -1.42178119 2.41681342
Ni 0.00469173 -0.06202015 1.17894341
Al -1.88233863 -1.42709711 -0.00837240
Al -1.85815679 1.34049031 0.00853029
Al 0.63565858 2.18555487 0.01497790
Al 0.76567638 -2.30550652 -0.01678654
Al 2.33871606 0.00048050 -0.00089943
Ni 0.00413053 -0.04723308 -1.18148256
Al -0.84632988 2.48512741 -2.49950614
Al -2.27312239 0.07658385 -2.42395873
Al -0.69603291 -2.26830869 -2.44642707
Al 1.74802053 1.43502077 -2.41030667
Al 1.91661256 -1.38594034 -2.43948752
Al -0.00403716 -0.04699994 3.95020062
Al -0.00565334 0.01005667 -3.95097773

19
dDh Ni Vertex

Al	0.16159000	-2.45066800	2.69448000
Al	1.55414900	1.98253200	2.79645900
Al	2.40899400	-0.61921200	2.85291000
Al	0.01252200	0.03736900	1.10544400
Al	1.88146100	1.78410600	0.00762000
Al	-0.21168400	-2.55447600	-0.03374700
Al	2.37289200	-1.02098400	0.05840300
Al	0.02398700	0.04429300	-1.35664400
Al	-0.61860700	-2.32432300	-2.82628900
Al	1.48618800	1.94157700	-2.74635700
Al	2.11714300	-1.23360100	-2.71057100
Ni	-0.10049900	-0.16481200	3.66781800
Ni	0.18841100	-0.01386200	-3.56858300
Al	-2.47287000	-0.30590100	-2.81169100
Al	-1.25032600	2.10276700	-2.76908400
Al	-1.56002900	2.11763500	0.02538800
Al	-2.48614800	-0.70253000	-0.00160600
Al	-2.44845100	-0.50342500	2.71883300
Al	-1.16204700	2.09351300	2.78058400

19
dDh$_{sp}$ Ni Vertex

Al	-2.25681082	-0.75931866	2.67050406
Al	-1.38878567	2.12649776	2.84263928
Al	0.55837918	-2.26042368	2.36005258
Al	1.32823147	2.13179184	2.77383628
Al	2.45539698	-0.34698134	2.79438968
Al	-0.01341630	0.24192288	1.20026148
Al	-2.54758417	-0.69852459	-0.05728038
Al	-1.74920642	2.12215134	0.05688384
Al	2.12755377	1.63030628	0.11779124
Al	-0.32846702	-2.61906374	-0.13045229
Al	2.30257330	-1.20015698	0.05624541
Al	-0.05825652	-0.02249035	-1.20868866
Al	-1.16284041	2.19994832	-2.63705592
Al	-2.42068986	-0.22910093	-2.85475162
Al	-0.69589812	-2.31782423	-2.85374555
Al	1.72572536	1.68686441	-2.56820343
Al	1.93752421	-1.51218901	-2.65951748
Ni	-0.06361690	-0.07166254	3.45255017
Ni	0.14686393	0.10825123	-3.47209172

19
Ih+Dh Ni Vertex

Al	-2.02685355	-1.32026791	2.53114485
Al	-1.88313135	1.52616737	2.52399258
Al	0.63658498	-2.33513265	2.53156694
Al	0.86681268	2.27011935	2.51869050
Al	2.42391895	-0.11617172	2.52526697
Al	0.00142549	-0.00072062	1.20742827
Al	-2.63520646	0.13082184	0.11632908
Al	-0.68945901	2.54541529	0.10616736
Al	2.20997796	1.44203899	0.10806773
Al	-0.93655360	-2.46760497	0.11906223
Al	2.05581504	-1.65511295	0.11533488
Al	0.00110365	-0.00091003	-1.20969013
Al	-0.62807444	2.32313946	-2.62416101
Al	-2.41063293	0.11796808	-2.61344220
Al	-0.86488133	-2.25794800	-2.61045431
Al	2.02137467	1.30902965	-2.62256674
Al	1.87331481	-1.52373004	-2.61479275
Ni	0.00396563	0.00747744	3.45941146
Ni	-0.00197919	-0.00839556	-3.49037672

19
Ih+Oh Pt Centre

Al	-2.51368831	0.27478394	2.72941838
Al	-0.58675377	2.37606959	3.23482536
Al	-0.62550391	-1.98256993	1.24020530
Al	2.01223958	1.67945669	2.71565387
Al	2.07192284	-1.00613329	2.37726147
Pt	-0.05110240	0.53274584	1.17715971
Al	-2.47183170	-0.13421523	0.07975194
Al	-1.87245355	2.54427390	0.84448721
Al	0.93623698	3.11886273	0.67102493
Al	1.82034627	-2.31460784	0.06742316
Al	2.23993659	0.57834438	-0.05655805
Pt	-0.07916833	-0.90343092	-1.16972413
Al	-0.29867603	1.71493109	-1.30044728
Al	-2.27541323	-0.34157401	-2.57836779
Al	-0.18121505	-1.71769533	-3.68784192
Al	1.77050979	0.44875003	-2.81214476
Al	2.15743164	-2.25840816	-2.55515640
Al	-0.12508670	-0.37939887	3.77158286
Al	-0.50888760	1.13733665	-4.08207381

19
Ih+Dh Pt Vertex

Al	-2.3671352	-1.0231117	2.6304362
Al	-1.8778140	1.8430473	2.7019237
Al	0.1727898	-2.2951230	2.6542263
Al	0.9979092	2.2991521	2.6542810
Al	2.2389946	-0.2587225	2.6738681
Al	-0.1618571	0.1225657	1.2096652
Al	-2.3131157	-1.2526765	-0.1371707
Al	-1.8853590	1.8061191	-0.2471451
Al	1.1658667	2.3104268	-0.1184077
Al	0.3910805	-2.6584874	-0.0855905
Al	2.6278215	-0.3718000	-0.0684455
Al	0.1031455	-0.1290558	-1.1860788
Al	-0.2795515	2.2820013	-2.6034524
Al	-2.3130793	0.1796655	-2.6140745
Al	-1.0155951	-2.3486422	-2.5563724
Al	2.2944760	1.0796769	-2.5258044
Al	1.8712018	-1.8157471	-2.6322759
Pt	-0.1715809	0.1119057	3.6659884
Pt	0.1278860	-0.1360834	-3.6039272